18TH WORLD CONFERENCE ON EARTHQUAKE ENGINEERING
WCEE2024
MILAN

MILAN, ITALY
30TH JUNE - 5TH JULY 2024
www.wcee2024.it

WAVE PROPAGATION IN LAYERED SOIL DEPOSITS

Roger D. Borcherdt[1]

US Geological Survey, Menlo Park, United States, rdborcherdt@gmail.com

Abstract: *Recent advances in the general theory of viscoelastic waves and rays in layered media provide a rigorous mathematical framework for site-specific, soil-response models used for earthquake resistant design. The advances provide general closed-form anelastic solutions for the classic problems of the response of a stack of soil layers to S and P waves, ray theory for reflected and refracted waves, Rayleigh- and Love-Type surface waves, and head waves. These general solutions valid for anelastic media regardless of the amount of material damping yield new insights regarding the characteristics of seismic waves and their ray paths that are not provided by conventional models. They provide corresponding numerical ground-response models and ray-tracing computation algorithms that account for changes in velocity and attenuation of anelastic waves associated with changes in inhomogeneity of the waves induced by anelastic soil and soil-rock boundaries. These anelastic effects manifest themselves as variations in amplitude response, amplitude attenuation, ray-path location, and travel time as observed at the Earth's surface. Implications of these anelastic effects for soil-response models used for earthquake resistant design are provided herein.*

1. Introduction

Intrinsic material damping plays a significant role in determining ground-motion amplitude estimates for purposes of earthquake resistant design (Kramer, 1996). The general constitutive theory of viscoelasticity provides an infinite number of phenomenological constitutive models that account for intrinsic material damping and the corresponding anelastic material behaviour of near-surface soil and rock deposits (Bland, 1960; Gurtin and Sternberg, 1962).

The general viscoelastic characterization of material behaviour has afforded closed-form theoretical solutions for the fundamental monochromatic problems of seismology pertinent to describing seismic wave propagation in soil and rock deposits. Theoretical viscoelastic solutions now exist for: P and two types of S body waves, reflection-refraction problems for single and multiple-layered media, Rayleigh- and Love-Type surface waves, Head waves, forward ray-tracing problems, ray-tracing computation algorithms for horizontal and spherical layered media with gradients, and simple inverse problems to infer intrinsic anelastic material absorption and wave speed from simultaneous measurements of travel time and amplitude (Borcherdt, 2020). The theoretical solutions reveal two types of anelastic S waves with distinct damping ratios and particle motions with that for Type II (SII) S waves being linear perpendicular to plane of propagation and attenuation and that for Type I (SI) S waves being elliptical in that plane.

Solutions of the reflection-refraction problem predict that seismic S and P waves refract across anelastic soil and rock boundaries as inhomogeneous waves with amplitudes that vary along surfaces of constant phase as illustrated in Figure 1. As a result, P and S wave characteristics such as wave speed (v_{HP}, v_{HS}), amplitude attenuation $(|\vec{A}_\phi|, |\vec{A}_\psi|)$, particle motion, directions of phase and amplitude propagation $(\vec{P}_\phi, \vec{P}_\psi; \vec{A}_\phi, \vec{A}_\psi)$,

and ray-path location vary with the degree of inhomogeneity (γ), angle of incidence (θ), and intrinsic material damping ratio $(DR = Q_{HP}^{-1}/2; DR = Q_{HS}^{-1}/2)$, This fundamental characteristic of waves in layered anelastic media manifests itself as changes in the response of a stack of soil layers to incident bedrock motions as well

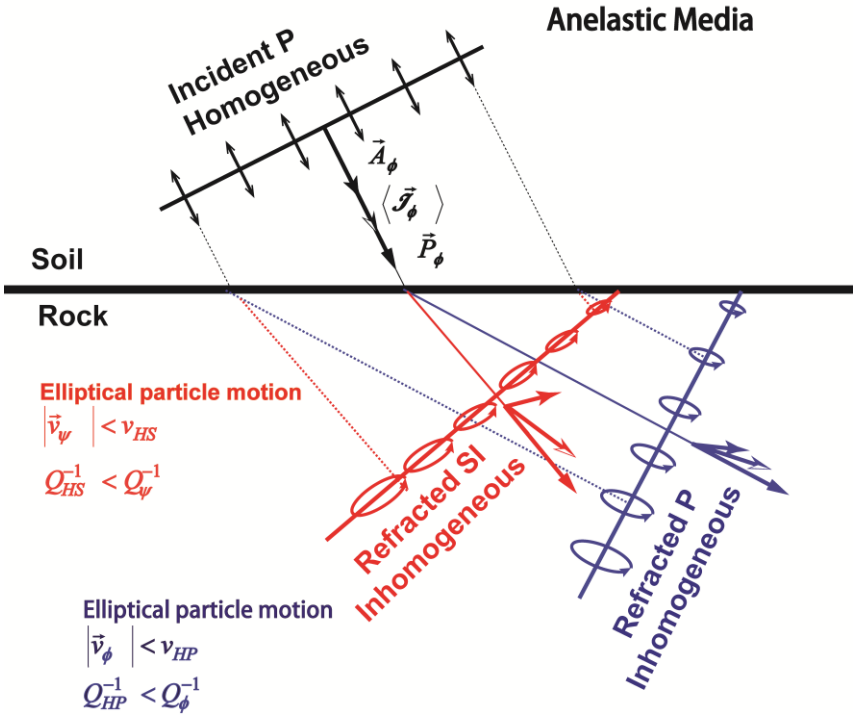

Figure 1. Diagram showing that contrasts in intrinsic material damping ratios and wave speed at anelastic soil-rock boundaries cause surfaces of constant amplitude and phase to refract in different directions with the resulting wave inhomogeneity changing with angle of incidence. This wave inhomogeneity manifests as reductions in wave speed, increases in wave damping, and elliptical particle motions for refracted P and SI waves (Borcherdt, 1982).

as changes in wave's ray paths with implications for the response of alluvial basins. The purpose of this paper is to provide examples that illustrate these manifestations.

2. Viscoelastic Response of Multiple Layers

The solution of the classic problem of the response of a stack of soil layers with damping to an incident SII (SH) wave has provided the theoretical basis to describe site-response estimates used for building code provisions and site-specific design purposes. This problem was first solved for the special case of homogeneous SH waves vertically incident on a stack of soil layers assumed to be Kelvin-Voigt solids overlying an elastic half space (Sezawa and Kanai, 1932; Kramer, 1996, p. 268). The general solution developed more recently is valid for general (homogeneous or inhomogeneous) SII waves incident at an arbitrary angle of incidence on a stack of soil layers overlying a half space, each of which may be modelled by any of an infinite number of viscoelastic constitutive laws (Borcherdt, 1977; 2009; 2020). This general solution of the classic soil response problem with appropriate adjustments in the intrinsic material parameters for stiffness and damping with strain levels provides the theoretical basis for a more detailed description of site response for site-specific engineering design purposes.

As a first example, the normalized amplitude responses for homogenous SII (SH) waves incident on a viscoelastic layer are shown in Figures 2a-d. These responses in each figure are computed for specific amounts of intrinsic material damping ratio values $(DR = Q_{HS}^{-1}/2)$ that range from those for near-elastic media (Fig. 2a) to low-loss Earth's crust (Fig 2b) and rock (Fig. 2c) to soil boundaries with large amounts of material damping (Fig. 2d). The responses are computed as a function of frequency normalized to the

fundamental frequency of the layer $(f\ /\ f_o)$ and as a function of the ratio of intrinsic material wave speeds (v_{HS_1}/v_{HS_2}).

The calculations illustrate that the amplitude response of the classic example for a normally incident homogeneous SII wave is frequency dependent with local maxima corresponding to the resonant frequencies

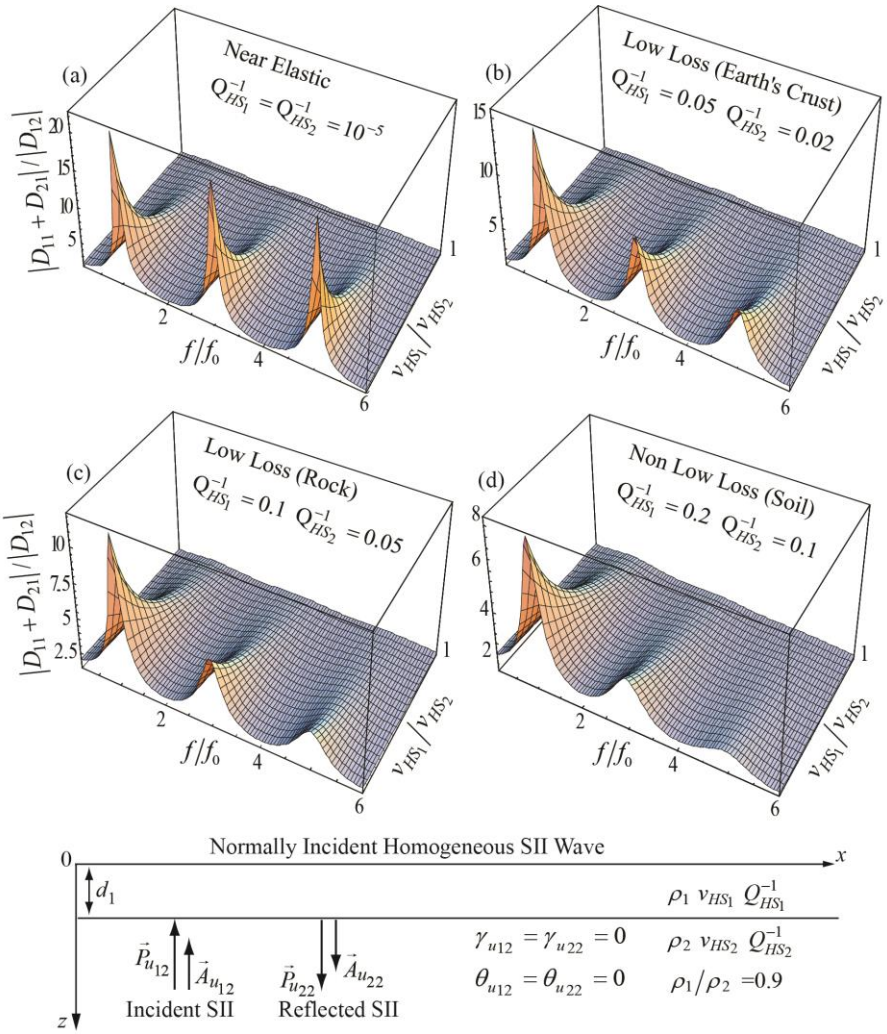

Figure 2. Amplitude response of viscoelastic layers to normally incident homogenous SII waves as a function of normalized frequency and the ratio of intrinsic material wave speeds of the layers with amounts of material damping ranging from that of the Earth's crust to that of rock and soil layers (from Borcherdt, 2020).

at the fundamental and higher modes which occur at odd multiples of $f_0 = v_{HS_1}/4d_1$ for materials with $v_{HS_1}/v_{HS_2} \leq 1$ and at approximately even multiples for $v_{HS_1}/v_{HS_2} \geq 1$. The figures indicate that the local maxima for elastic media are independent of frequency, but their dependency on frequency for anelastic media increases as the intrinsic material damping of the layer increases.

To illustrate the influence of inhomogeneity and angle of incidence on the response of a firm soil layer overlying a rock layer, responses for an incident SII wave with various amounts of inhomogeneity $(\gamma_{u12} = 0, -60^o, -80^o, -86^o)$ are shown in Figures 3a-d as a function of angle of incidence. For near-vertical angles of incidence the response for a homogeneous wave (Fig 3a) is dominant at vertical incidence and that for an inhomogeneous wave (Figs. 3b, 3c,3d) decreases with increasing inhomogeneity of the incident anelastic SII wave. For larger shallow angles of incidence, the response of inhomogeneous waves (Figs. 3b, 3c, and 3d) for the fundamental and higher modes show notable increases. These increased responses

increase with inhomogeneity of the incident wave. These increased responses for incident inhomogeneous waves at shallow angles of incidence are not predicted by the classic vertically incident homogeneous SH soil response model.

To better illustrate the implications of seismic wave inhomogeneity for engineering applications, the results for a vertically incident homogenous wave in Fig. 3a are replotted as a function of period in Figure 4 for intrinsic

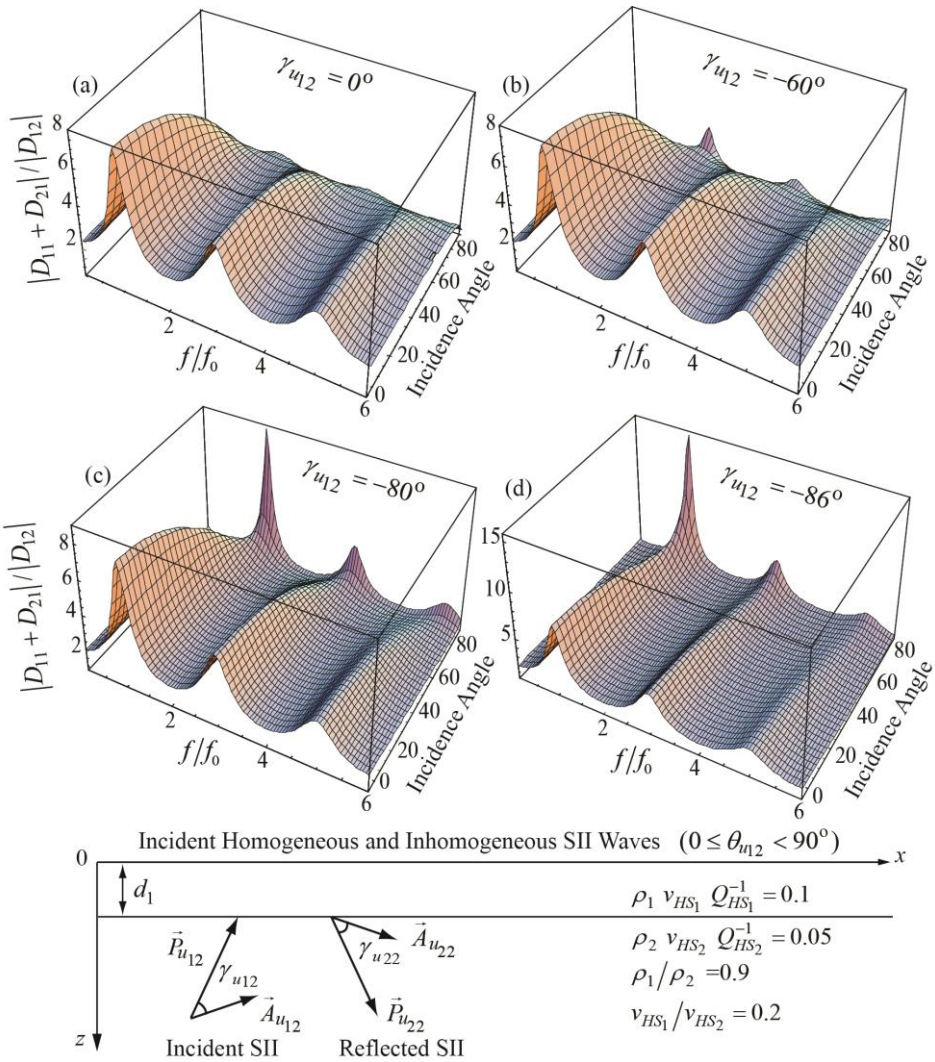

Figure 3. Amplitude response of a viscoelastic layer as a function of normalized frequency and angle of incidence for incident SII anelastic waves with degrees of inhomogeneity of $\gamma_{u12} = 0^o, -60^o, -80^o, -86^o$ *(from Borcherdt, 2020).*

material damping ratios of 5 % and 20 % that correspond to approximate input base acceleration levels of 0.1 g and 0.5 g. (These response values correspond to those that could be calculated for an incident S wave using the SHAKE program (Schnabel, et al, 1972]). Approximate site-class boundaries as inferred from the material velocity ratios shown in Fig. 3a and corresponding average site coefficients Fa and Fv are superimposed as specified in the 1994-2009 NEHRP provisions for new buildings (Borcherdt, 1994). These plots illustrate that the theoretical viscoelastic model predictions for a normally incident SII wave can be used to account for the principal characteristics of average site response factors as well as more detailed spectral estimates of site coefficients for use in site-specific design estimates and building code provisions.

To provide additional insight regarding the effects of inhomogeneity, the response of a site-class E soil layer $(V_{S30} = 180\ m/s)$ with a damping ratio of 10 % is calculated as a function of angle of incidence for incident homogeneous and inhomogeneous Type-II S waves (Figure 5). (These response estimates with a damping ratio of 10% instead of 5% computed as a function of period correspond to those calculated as a function of

frequency in Fig 3a and Fig 3d. The response for an incident homogenous wave (Fig. 5a) shows that the responses at the fundamental and higher modes are largest for vertical angles of incidence then decrease with increasing angles of incidence. The response for the case of an incident inhomogeneous wave Fig. 5b shows that the maximum amplitudes that occur at the periods of the fundamental and higher modes increase with angle of incidence. This increased response could contribute to an increase in the response of some alluvial basins near basin margins.

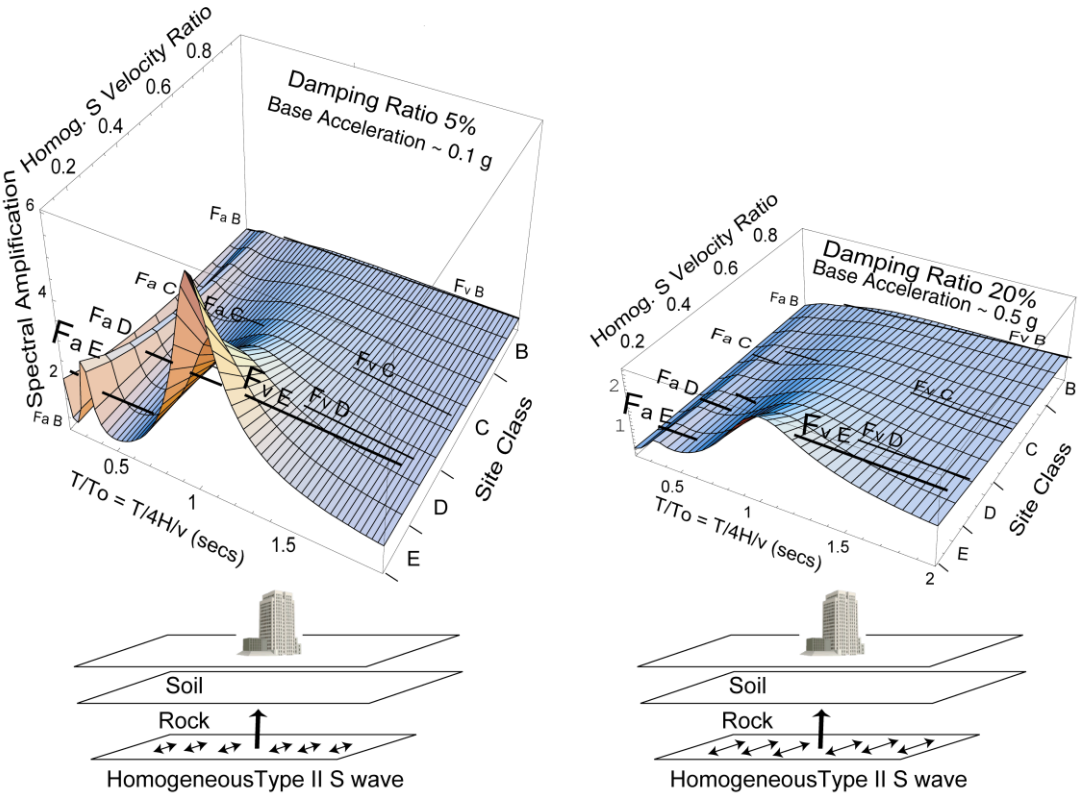

Figure 4. Amplitude response of a soil layer to vertically incident anelastic homogeneous SII waves as a function of normalized period and intrinsic material wave velocities of the layers for damping ratios of 5% and 20%. Corresponding scale for site classes and average short- and mid-period (Fa, Fv) NEHRP site coefficients.

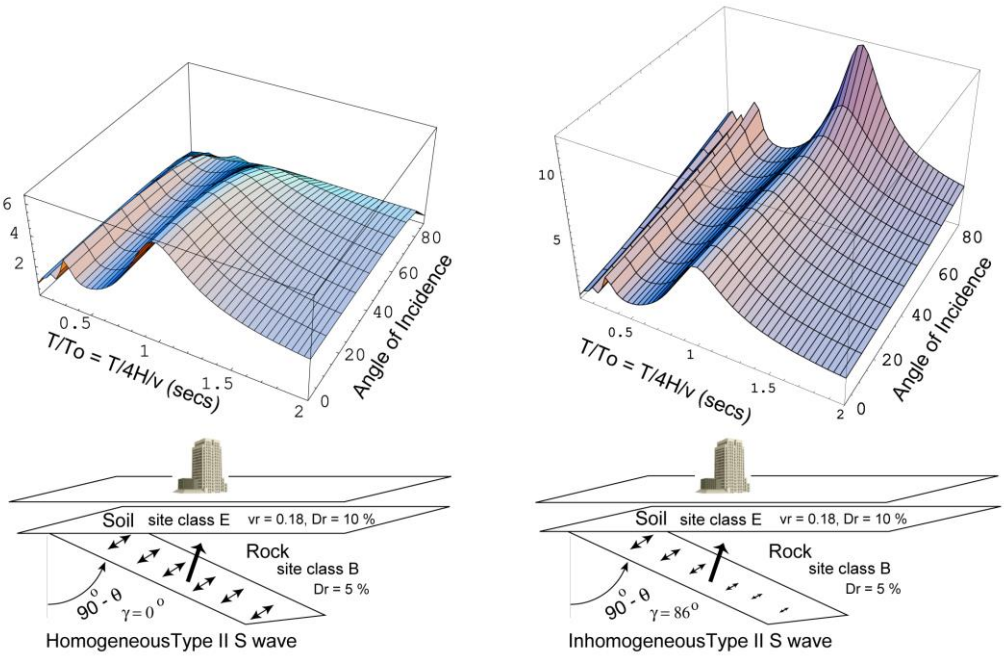

Figure 5. Amplitude response of viscoelastic site-class E $(v_{S30} = 180\,m/s; Dr = 10\%)$ *soil layer as a function of normalized frequency and angle of incidence for incident SII waves with degrees of inhomogeneity of* $\gamma = 0^{o}, -86^{o}$.

The closed-form theoretical viscoelastic solutions for general (homogeneous or inhomogeneous) SII waves incident on a stack of anelastic layers as parameterized herein provide exact numerical response models that account for the effects of inhomogeneity of seismic waves as induced by contrasts in intrinsic material damping at soil and rock boundaries. The results confirm that the classic site-response problem for vertically incident homogenous SII waves on a stack of soil layers with material damping adjusted to appropriate strain levels provides a conservative estimate of site response for near-vertical angles of incidence for site-specific engineering design purposes. However, for shallow angles of incidence the results show that inhomogeneity of the incident wave can result in increased amplification for shallow angles of incidence. To account for this situation conservative estimates of site response will need to account for angle of incidence and inhomogeneity of the incident wave, which in practice may need to be considered only for those situations that merit extensive modelling efforts.

3. Implications of Viscoelastic Ray Theory

Recent developments in general viscoelastic ray theory provide a rigorous mathematical framework for anelastic seismic tomography of layered near-surface media of interest for geotechnical engineering as well as the Earth's deep interior (Borcherdt, 2020, pp. 276-432; 2023 in press). They provide closed-form solutions of forward ray-tracing and simple inverse problems for anelastic horizontal and spherical layered media with material gradients. They provide ray-tracing computation algorithms valid for all angles of incidence, that account for changes in wave speed, attenuation, and trajectory of anelastic P and S body waves as induced by anelastic boundaries.

Fundamental distinctions between elastic and anelastic viscoelastic ray paths are illustrated in Figure 6 for SII waves in a stack of horizontal layers with monotonic anelastic intrinsic-material parameters. At elastic boundaries P and S waves refract as homogenous waves with parallel directions of phase and amplitude propagation. Their wave speed in each layer is unique and does not vary with angle of incidence. At anelastic boundaries, P and S waves refract as inhomogeneous waves with directions of phase propagation and maximum attenuation dependent on the angle of incidence and the contrast in material damping as illustrated in Fig.1. As a result, their wave speed and attenuation is not unique and varies with angle of incidence and the degree of inhomogeneity of the wave as induced at each anelastic boundary traversed by the wave. Their wave speeds are less than that of the intrinsic-material wave speed for corresponding homogenous waves.

Hence, anelastic rays refract at steeper angles of refraction than elastic rays. As a result, the path length, surface distance, travel time, and amplitude attenuation along anelastic ray paths can be larger than that for elastic ray paths for homogenous waves.

A problem of interest is the effect that contrasts in intrinsic material damping and wave field inhomogeneity may have on the amplification of seismic waves at various locations in an alluvial basin. Application of the viscoelastic ray-tracing computation algorithms to horizontal layered structures provides an opportunity to gain some insight on this problem. Toward this objective, the algorithms as coded in computer program (VRAYS) are used to trace the reflection and refraction of SII waves in a simplified four-layer geotechnical model of soil and rock as illustrated in Fig. 6. The simplified model is comprised of a stack of two soil layers underlain by layers of soft and firm rock with intrinsic material shear-wave-speed and damping-ratio profiles as indicated in Figure 7. Material parameters for the layers are derived from borehole S and P wave velocity logs (Gibbs et al, 1994) at sites of the "*Integrated Strong-motion Array* "in San Francisco, CA (Borcherdt et al., 2005). Material parameters for the layers in the model are chosen to correspond to those for Younger Bay Mud (YBM), Older Bay Sediments (OBS), Soft Rock (SR), and Firm Rock (FR).

Travel times and normalized amplitudes for SII-wave ray paths emanating from the surface and reflecting back to the surface from the base of the first, second, and third layers are shown as a function of angle of incidence in Figure 8. Results are shown for both elastic and anelastic ray paths with those for anelastic ray paths computed for damping ratio estimates of 5, 10, and 20 percent for the Younger Bay Mud (YBM) surface layer and fixed damping ratios of 2.5, 2, and 1.7 percent for the successively deeper layers. The damping ratios for the YBM layer correspond roughly to input ground motion levels that might range from 0.1g to 0.5 g.

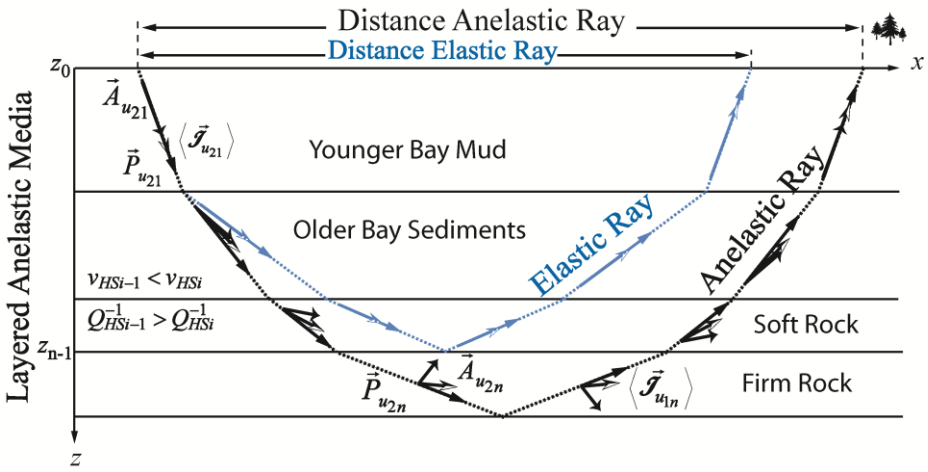

Figure 6. Diagram illustrating distinct ray paths for elastic and anelastic waves in a stack of horizontal layers.

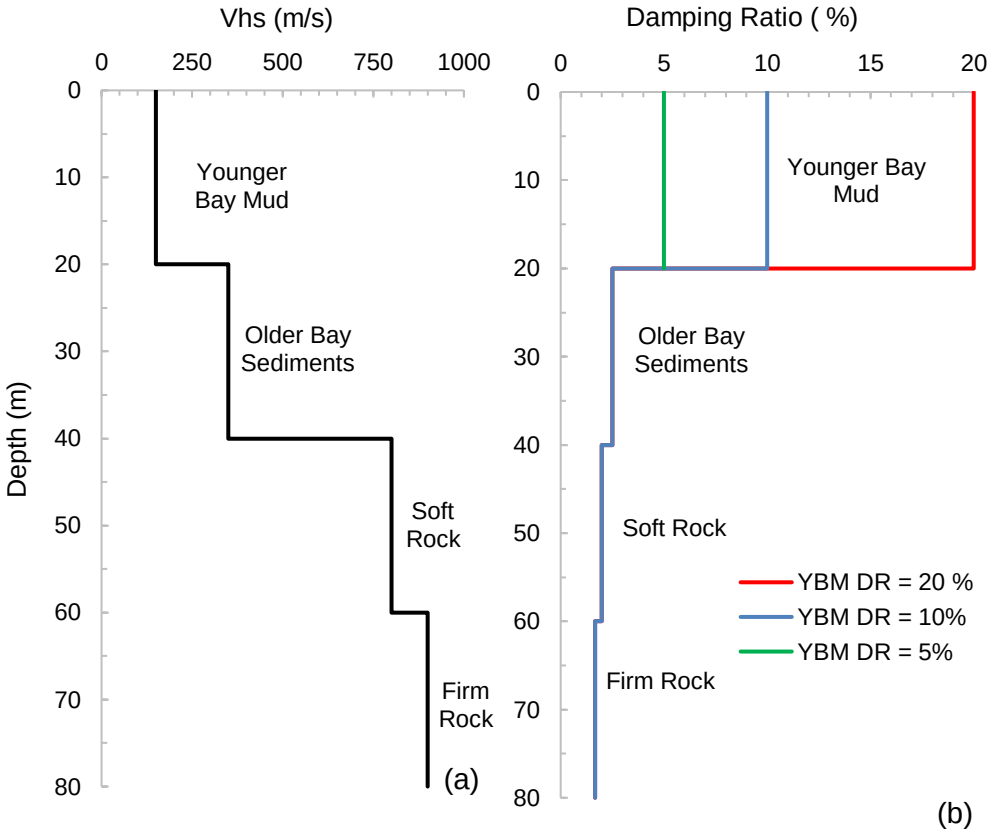

Figure 7. Intrinsic material wave speed and damping ratio profiles for a simplified four-layer geotechnical model comprised of layers of Younger Bay Mud, Older Bay Sediments, Soft Rock, and Firm Rock.

The travel times and amplitudes for the ray paths reflected from the Younger Bay Mud-Older Bay Sediment boundary are shown in Figs 8a and 8b. The travel times for the reflection of the assumed incident homogeneous wave from the base of the first layer (Fig. 8a) do not show a discernible difference between that for elastic or anelastic ray paths with various amounts of intrinsic material absorption. This result is as would be expected, because the incident homogeneous wave reflects as a homogeneous wave both in elastic and anelastic media. However, comparison of the reflected amplitudes (Fig. 8b), shows significant distinctions between those for elastic and anelastic models as well as those with varying amounts of intrinsic absorption. The elastic model predicts that total reflection occurs for all angles of incidence greater than or equal to the critical angle. The reflections from the base of the YBM layer indicate that for the head-wave critical angle and

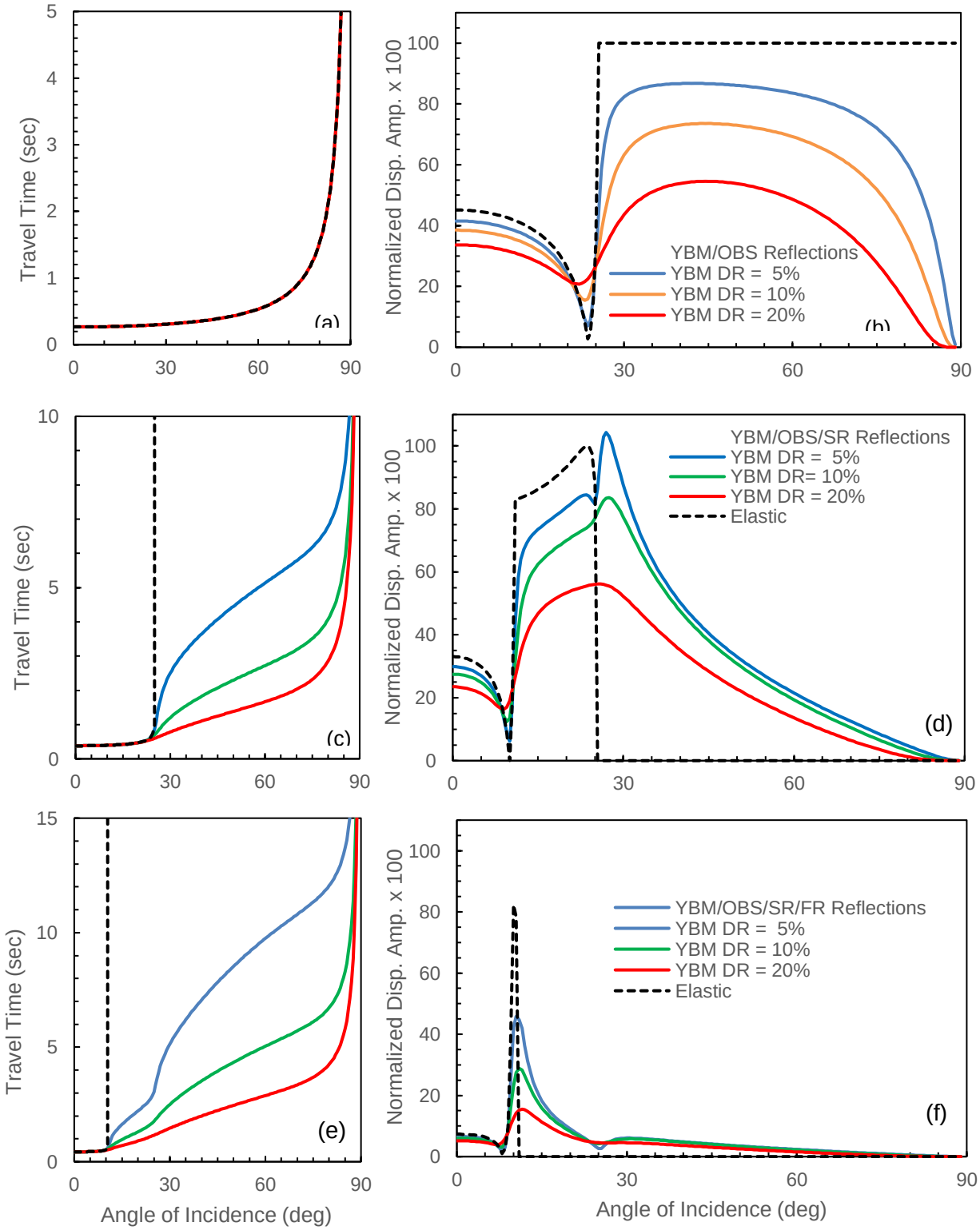

Figure 8. Travel-time and amplitudes for SII rays emanating from the surface and reflecting back to the surface from the base of the first, second, and third layers as a function of angle of incidence for models with damping ratios of 5%, 10%, and 20% for the Younger Bay Mud (YBM) layer.

for wide angles of incidence significant amounts of energy are not reflected back to the surface, but instead transmitted across the boundary as Wide-Angle Refracted (WAR) waves, which the elastic model predicts do not exist.

Further insight into the nature of the anelastic WAR waves is provided by utilizing the exact viscoelastic computation algorithms to infer the travel times and amplitudes for the corresponding rays transmitted across the YBM-OBS boundary then reflected from the OBS-SR boundary and transmitted back to the surface. These travel time and reflected amplitude profiles are shown in Figs. 8c and 8d. The travel time curves become

discernibly distinct only for the critical angle and wide angles of incidence. The elastic model predicts that the ray path and travel time for the refracted wave that reflects from the second boundary becomes infinite as the angle of incidence approaches the elastic critical angle. In contrast, the anelastic model predicts well-defined travel time curves for the reflected inhomogeneous WAR waves.

The travel time curves at wide angles of incidence (Fig. 8c) show a strong dependence on the intrinsic material absorption or damping ratio of the Younger Bay Mud surface layer. These distinctions in the travel times for the reflected WAR waves associated with differences in the material damping ratio are due to changes in the length of the travel path caused by changes in the directions of phase propagation for the refracted waves as induced by the contrast in intrinsic absorption at the boundary. These predicted changes in trajectory of seismic waves caused by contrasts in anelastic boundaries have been predicted for other anelastic boundaries, such as those in ocean-bottom sediments, crust, and mantle. These distinctions suggest that travel time measurements for models such as these could be useful for inferences regarding intrinsic material absorption as well as intrinsic velocity structure.

The amplitude curves for reflections from the Older Bay Sediment-Soft Rock boundary (Fig. 8d) reveal distinct variations associated with the intrinsic damping ratio of the YBM layer and the resulting contrast in intrinsic damping across the boundary. The elastic model predicts that no energy is reflected for wide angles of incidence beyond the elastic critical angle (~27^O). The anelastic model predicts that the largest reflected amplitudes occur for the reflected WAR waves at wide angles of incidence with significant amplitudes for a relatively broad range of larger incident angles. The reflected amplitudes show well-defined distinctions for all angles of incidence associated with the intrinsic material damping ratio of the YBM surface layer. The curves reveal significant amounts of energy are transmitted across the YBM-OBS boundary at wide angles of incidence then subsequently reflected from the anelastic boundary at the base of the OBS layer beyond the elastic critical angle. The calculations show that the amplitudes of the reflections from both the YBM and OBS boundaries depend on the material damping ratio for the YBM layer. They also reveal that the elastic critical angle for the second (OBS-SR) boundary occurs at an angle of incidence for the incident ray from the surface of about 10^O.

Additional insight regarding the effects of anelastic WAR waves on travel times and amplitudes of seismic waves is provided by considering their subsequent reflection from the Soft Rock-Firm Rock boundary. These calculations are provided in Figs. 8e and 8f. The travel times show distinct variations for angles of incidence greater than the critical angle of 10^O for the preceding OBS-SR boundary. These variations increase with angle of incidence to the critical angle of 26^O for the preceding YBM-OBS layer at which point an increase in the slopes of the travel-time curves is apparent especially for the curves corresponding to damping ratios of 5 and 10 %. The travel-time curves provide evidence of WAR waves induced by both of the anelastic boundaries encountered along the ray path.

The reflected amplitude curves for the SR-FR boundary reveal that the largest amplitudes occur for waves refracted at angles of incidence greater than the critical angle of 10^O for the preceding OBS-SR boundary. The curves provide evidence of anelastic WAR waves induced by the contrast in intrinsic material absorption at the previous boundary. The curves also reveal a minor but local maximum associated with the maxima in WAR wave amplitudes induced near 28^O by the first YBM-OBS anelastic boundary. The amplitude curves show a well-defined dependence on the amount of intrinsic material damping in the YBM layer.

The travel times and amplitudes calculated for the four layer model indicate that anelastic boundaries can induce significant changes in the trajectory, wave speed, amplitude, attenuation, and ray path for seismic waves refracted at wide angles of incidence in soil rock layers that are not predicted by elastic ray theory models. The results calculated here for the four-layer geotechnical model provide additional confirmation of those computed for other ocean- bottom, crust, and mantle models (Borcherdt, 2023, in press). These results predict the existence of WAR waves in alluvial basins with trajectories, ray paths, travel times, and amplitudes that imply changes in the amount and location of basin amplification that are not predicted by elastic models.

4. Conclusions

Recent advances in the general theory of viscoelastic waves and rays in layered media provide a rigorous mathematical framework for site-specific, soil-response models used for earthquake resistant design. They provide corresponding numerical ground-response models and ray-tracing computation algorithms that account for changes in velocity and attenuation of anelastic waves associated with changes in inhomogeneity of the waves induced by anelastic soil and soil-rock boundaries. They predict that seismic waves refract across anelastic boundaries for all angles of incidence. They account for energy carried by plane waves along seismic boundaries at head-wave critical angles and Wide-Angle Refracted (WAR) ray paths that are not predicted by elastic models.

Recent general solutions developed for the classic problem of a stack of soil layers with damping to vertically incident elastic SH waves extend the theoretical solutions to include homogeneous or inhomogeneous SII waves incident at an arbitrary angle of incidence on a stack of layers with any of an infinite number of possible viscoelastic constitutive models of intrinsic material damping and wave speed. These general solutions with appropriate adjustments in the intrinsic material parameters for strain level provide the theoretical basis for numerical models to evaluate the effects of angle of incidence, intrinsic material damping, and wave-field inhomogeneity on site response estimates for site-specific engineering design purposes.

Numerical estimates of site response based on the general solution confirm that vertically incident homogenous SII waves on a stack of soil layers with material damping adjusted to appropriate strain levels provide a conservative estimate of site response for near-vertical angles of incidence for site-specific engineering design purposes. For shallow angles of incidence, the general solution results show that inhomogeneity of the incident wave can result in increased amplification. To account for this situation conservative estimates of site response will need to account for angle of incidence and inhomogeneity of the incident wave, which in practice may need to be considered only for those situations that merit extensive modelling efforts and be of significance for certain basin geometries.

Recent advances in general viscoelastic ray theory provide a new mathematical framework to trace seismic rays in an anelastic Earth. Closed-form solutions of the forward ray-tracing problems for horizontal and spherical anelastic media account for changes in velocity and attenuation along anelastic P and S wave ray paths that are not encountered along elastic paths (Borcherdt, 2020).

Recent developments in general viscoelastic ray theory provide a rigorous mathematical framework for site-response estimates and anelastic seismic tomography of layered near-surface soil and rock deposits of interest for geotechnical engineering (Borcherdt, 2020, pp. 276-432; Borcherdt, 2023 *in press*). These developments include exact ray-tracing computation algorithms valid for inhomogeneous P an S waves incident at all angles of incidence in layered soil and rock deposits.

Application of these algorithms to a four layer model comprised of Younger Bay Mud, Older Bay Sediments, Soft Rock, and Firm Rock reveal that the anelastic boundaries between these layers can induce significant changes in the trajectories, travel times, and amplitudes of seismic waves refracted at wide angles of incidence. The numerical results confirm the existence of wide-angle refracted (WAR) waves with travel times and significant amplitudes that are not predicted by conventional elastic ray-tracing algorithms. Calculations also reveal that the travel paths, travel times, and amplitudes for WAR waves reflected from successively deeper boundaries depend strongly on the intrinsic material damping ratio of the surface layer. This dependence can manifest as changes in the amount and location of amplification anomalies in alluvial basins.

These recent preliminary findings regarding reflected inhomogeneous WAR waves and their dependence on intrinsic material damping appear to have significant implications for interpretations of seismic reflection and refraction profiles as well as for the prediction of local amplification anomalies in alluvial basins. The results suggest additional investigations are warranted. A current challenge is the incorporation of the recent developments in viscoelastic wave-propagation and ray theory into inversion and prediction procedures for layered anelastic near-surface, crust, and mantle materials in the Earth.

5. Acknowledgments

The review comments of Dr. Joe Fletcher are appreciated. The author's VRAYS viscoelastic ray-tracing Fortran code provided the numerical arrays for graphs prepared with EXCEL. Gary

Glassmoyer's initial program assistance and Larry Baker's recent computer advice are gratefully acknowledged. The author acknowledges that no conflicts of interest are recorded.

6. References

Bland, D.R. (1960). *The Theory of Linear Viscoelasticity*, New York, Pergamon Press.

Borcherdt, R. D. (1977). Reflection and refraction of Type-II S waves in elastic and anelastic media, *Bull. Seismol. Soc. Am.*, 67, 43-67. Google Scholar

Borcherdt, R. D. (1982). Reflection-refraction of general P- and Type-I S waves in elastic and anelastic solids, Geophys. *J. R. Astron. Soc*., **70**, 621-638, doi: 10.1111/j.1365-246x.1982.tb05976. Google Scholar

Borcherdt, R.D. (1994). Estimates of site-dependent response spectra for design (Methodology and Justification, *Earthquake Spectra*, 10: 617-653. Google Scholar

Borcherdt, R.D., (2009). *Viscoelastic Waves in Layered Media*, Cambridge University Press. doi: https://doi.org/10.1017/CBO9780511580994

Borcherdt, R.D., (2020). *Viscoelastic Waves and Rays in Layered Media*, 2nd Ed., Cambridge University Press. doi: https://doi.org/10.1017/9781108862660

Borcherdt, R.D. (2024, *in press*). Preliminary implications of viscoelastic ray theory for anelastic seismic tomography models, submitted 9/15/2023, Special Issue "Modern Seismic Tomography", *Bulletin Seismological Society of America.*

Borcherdt, R.D., Glassmoyer, G., Dietel, C., and Westerlund, R. E. (2005). Integrated Surface and Borehole Strong-Motion, Soil-Response Arrays in San Francisco, California, in book *Directions in Strong Motion Instrumentation*, researchgate

Gibbs, J.F., Fumal, T.E., Borcherdt, R.D., Warrick, R.E., Liu, H., and Westerlund, R.E. (1994). Seismic velocities and geologic logs from boreholes at three downhole arrays in San Francisco, California: U.S. Geological Survey Open-File Report 94–706, 40 p. https://pubs.usgs.gov/of/1994/0706/.

Gurtin, M. E. and Sternberg, E. (1962). On the linear theory of viscoelasticity, *Archive of Rat. Mech. Analysis*, **II**, 291-356.

Kramer. S.L. (1996). *Geotechnical Earthquake Engineering*, Prentice-Hall, Upper Saddle River, New Jersey.

NEHRP *Recommended Provisions for Seismic Regulations for New Buildings* (1995) *FEMA 222A / 1994 Edition.*

NEHRP Recommended Seismic Provisions for New Buildings and Other Structures (2009) *FEMA P-750 / 2009 Edition.*

Schnabel, P.B., Lysmer, J., and Seed, H.B. (1972)."SHAKE - A Computer Program for Earthquake Response Analysis of Horizontally Layered Sites". Earthquake Engineering Research Center, UCB/EERC-1972; 72/12: University of California, Berkeley.

Sezawa K. and Kanai, K. (1932). Reflection and refraction of seismic waves in a stratified body. Bull. Earthq. Res. Inst. Tokyo Imp. Univ. 10(4):805–816.